# Multi-Quantum Well (MQW) GaAs/AlGaAs Solar Cell

Omar Kazi
*Department of Electrical and Computer Engineering*
*University of Illinois at Urbana-Champaign, Urbana, IL 61801, USA*

(Completed 2 May 2021)

**Abstract**

Solar photovoltaic technologies have garnered an increasing amount of attention due to their relevance to developing sustainable energy systems in the future which do not harm the environment. Multi-quantum well (MQW) solar cells offer a potential device structure which can improve the current generation and efficiency of conventional p-i-n junction solar cells. Typically, only photons with energies matching or exceeding that of the bandgap of a solar cell can be absorbed to convert the irradiated light into an electrical current. Photons with less energy than the bandgap are not able to excite free charge carriers, which in effect reduces the efficiency of a solar cell. Layered quantum well structures in place of the intrinsic region of a solar cell could potentially harness these lower energy photons to generate current from charge carriers confined within those quantum wells. In this study, a single-junction MQW GaAs solar cell structure using 13 GaAs/$Al_{0.35}Ga_{0.65}As$ quantum wells is proposed and simulated using Crossslight APSYS (TCAD software). The structure of the quantum well region is optimized by investigating the effects of the $Al_{0.35}Ga_{0.65}As$ barrier thickness and the GaAs quantum well thickness on the device performance. The optimized cell efficiency is found to be 7.636% when 50 nm quantum wells and 1 nm barriers are used. This performance provides insights into how tunneling can reduce the performance of a MQW from its maximum theoretical efficiency and the trade-off between the thickness of the barriers and wells to design an optimal solar cell configuration.

## I. Introduction and Motivation

Fossil fuel energy sources have been causing an increasingly concerning level of damage to the environment in the form of greenhouse gas emissions contributing to global climate change. The impact of climate change on society is monumental and is already being observed as natural ecosystems are ravaged and sea level elevation threatens coastal civilizations. Therefore, there is great attention being devoted to sustainable and renewable sources of energy, of which solar photovoltaics offer the greatest potential to compete with fossil fuels. Unlike fossil fuels which are finite and need to be mined through environmentally destructive processes, solar energy is freely available in abundance. The energy irradiated from the sun onto the earth in the form of light in a single hour exceeds the annual energy demand of humans across the planet [1]. Therefore, the ability to effectively convert sunlight into usable forms of energy without causing environmental harm make photovoltaics an extremely potent technology to eliminate societal reliance on fossil fuels.

The current solar cell technology which is the most widespread is based on silicon materials, accounting for over 95% of the solar modules which are sold today [2]. This is due to a conglomerate of factors, including the high abundance and low cost of silicon as a material, as well as the relatively high efficiency (on the order of 25%) and long lifetime (at least 25 years) of silicon solar cell modules. Silicon is also a material used commonly in the fabrication of other semiconductor devices such as transistors and integrated circuits, making it an easier material to work with due to the existence and availability of well-established manufacturing and processing techniques. However, despite their popularity, silicon solar cells are not the most efficient single-junction solar cells available. This accolade instead belongs to GaAs solar cells, which have recorded efficiencies as high as 28.8% under the illumination of a single sun [3].

GaAs has a bandgap of 1.42 eV, which is very close to the peak emitted photon energy of the AM1.5 solar spectrum (Figure 1). The AM1.5 spectrum is often the standard solar spectrum used to evaluate the performance of flat-plane solar modules for terrestrial applications. Thus, due to its bandgap and its high absorption coefficient, a GaAs cell is able to convert the energy of more solar photons than conventional silicon cells. Although GaAs surpasses silicon in its efficiency, GaAs is a far less abundant and more costly material than silicon, making the average cost of a GaAs solar module higher than that of silicon. The efficiencies of these solar cells can significantly be increased by designing multijunction solar cells which make use of layers of cells with different wavelength regimes of absorption. However, this also results in increased cost and complexity compared to single-junction cells. GaAs and other solar cells which integrate group III-V semiconductor materials have typically been more popular in niche applications such as space exploration where the need for high efficiency and performance outweighs the restrictions of cost or toxicity.

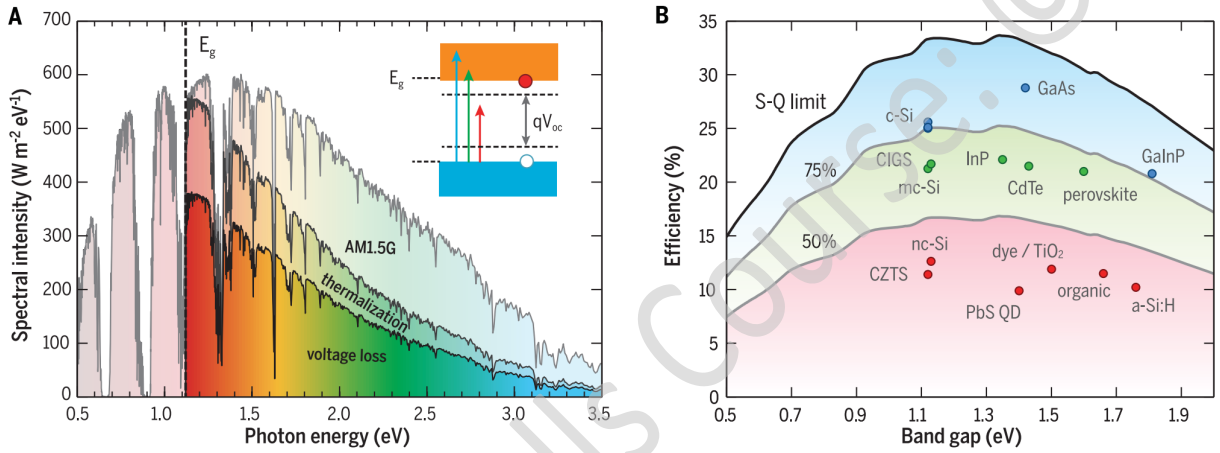


**Figure 1.** (**A**) *The spectral intensity of the AM1.5 solar spectrum plotted as a function of photon energy, with indications of the bandgap and absorption in silicon.* (**B**) *The theoretical Shockley-Queisser limit of efficiency for solar cells of various materials as a function of their band gap energies* [3].

The multi-quantum well solar cell is a technology which has been studied for several decades as a method of improving the efficiency of conventional single-junction solar cells. The inclusion of quantum wells can allow some photons of energy below the bandgap to still be absorbed and converted into a usable electric current, thus enhancing the overall conversion efficiency of a solar cell [4]. Therefore, it is of great interest to implement this design for GaAs solar cell systems in an attempt to develop single-junction solar cells with efficiencies above 30% and eventually approach the Shockley-Queisser limit of efficiency. In this study, a potential design for a multi-quantum well GaAs/AlGaAs solar cell is modeled using technology computer-aided design (TCAD) simulations in the Crosslight APSYS software.

## II. Technical Background

A solar cell is a semiconductor device which can convert light irradiated by the sun into electrical energy. This occurs by the excitement of electrons in a semiconductor material from the valence band to the conduction band when the absorbed photons supply enough energy for the electron to cross the associated energy barrier. This results in the presence of free electrons in the conduction band and free holes in the valence band. In a solar cell, a p-n junction is present in the active region so that electrons and holes which are freed during light absorption can move across the junction to generate a current, called a photocurrent (Figure 2). This process is called the "photovoltaic effect", which is distinct from the effect observed if a material is photoconductive. While both can potentially exhibit electronic responses when

illuminated, a photovoltaic material can generate a current without the application of an external bias from another power supply.

The energy which is required for an electron to be promoted from the valence band to the conduction band is known as the bandgap energy ($E_g$). If a photon with energy $E \geq E_g$ is incident upon a system exhibiting the photovoltaic effect, then electrons can be promoted from the valence band to the next highest discrete energy level (i.e., the conduction band). Any excess energy above the bandgap is lost as heat (thermalization), which is an undesirable process. If an incident photon has energy $E < E_g$, then it simply passes through the material without being absorbed because it has insufficient energy to promote an electron from the valence band to the next highest discrete energy level (Figure 3). In an ideal solar cell system, the bandgap structure should be designed to absorb as many photons emitted in the solar spectrum as possible to harness the greatest amount of energy and in effect achieve the highest efficiency.

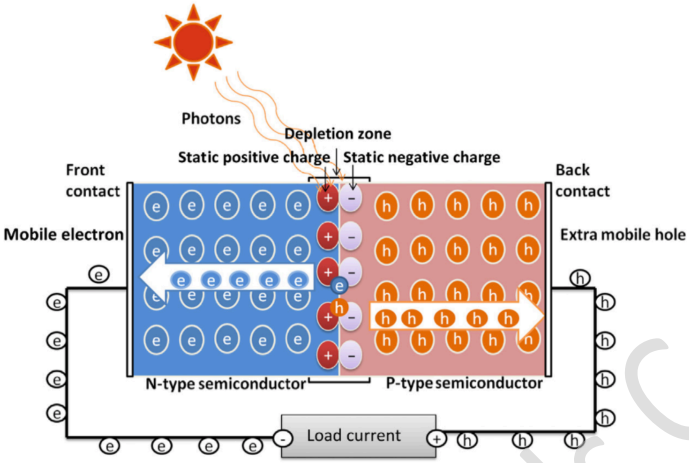


**Figure 2.** *Schematic of a p-n junction exhibiting the photovoltaic effect to generate a current when sunlight is incident upon it* [5].

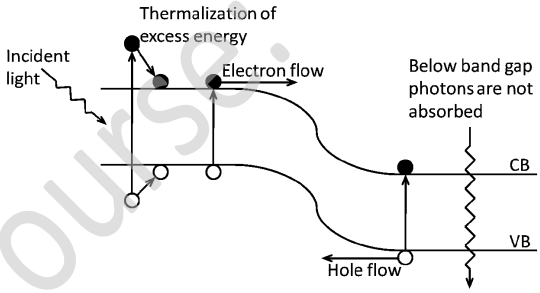


**Figure 3.** *Band (energy) diagram of a p-n junction exhibiting the photovoltaic effect and demonstrating the effects for incident photon energies greater than or less than the bandgap energy* [6].

A solar cell can be modeled through an equivalent circuit involving a single diode, which is aptly named the single diode model (Figure 4).

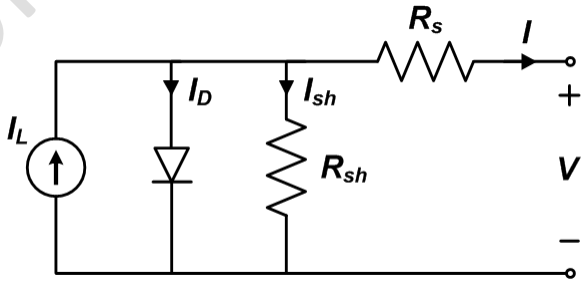


**Figure 4.** *Equivalent circuit of a solar cell following the single diode model* [7].

In this circuit, $I_L$ represents the current generated by light (i.e., by the photovoltaic effect) in the cell, $I_D$ is the current lost due to electron-hole recombination in the cell, and $I_{sh}$ is the current lost to the shunt resistance. In this model, the current through the diode, $I_D$, can be expressed using the Shockley equation for an ideal diode:

$$I_D = I_0\left[e^{\frac{V+IR_S}{nV_T}} - 1\right]$$

In the Shockley diode equation, $n$ is the diode ideality factor, $I_0$ is the saturation current, and $V_T$ is the thermal voltage which can be expressed as:

$$V_T = \frac{k_B T_c}{q}$$

By applying Kirchoff's current law, the equation for the overall current outputted by the solar cell can be calculated as:

$$I = I_L - I_D - I_{sh} = I_L - I_0\left[e^{\frac{V+IR_S}{nV_T}} - 1\right] - \frac{V + IR_S}{R_{sh}}$$

Two of the important metrics for solar cells which can be extracted using the single diode equivalent circuit model include the short circuit current ($I_{sc}$) and the open circuit voltage ($V_{oc}$). The short circuit current corresponds to the current ($I$) when the voltage is set to zero ($V = 0$) and the open circuit voltage corresponds to the value of $V$ when $I = 0$. These can also be observed on the IV curve of a solar cell as the intercepts on their respective axes (Figure 5). These parameters are necessary in order to determine the fill factor (*ff*) of a solar cell, which represents the ratio of the maximum power point (MPP) to the product of $V_{oc}$ and $I_{sc}$.

$$ff = \frac{P_{max}}{V_{oc}I_{sc}} = \frac{V_{MPP}I_{MPP}}{V_{oc}I_{sc}}$$

A higher fill factor is indicative of a higher quality and more efficient solar cell. However, the fill factor is not the same as efficiency; rather, the efficiency is defined as the ratio of the maximum power of the solar cell to the power incident upon it in the form of irradiated sunlight:

$$\eta = \frac{P_{max}}{P_{incident}} = \frac{V_{oc}I_{sc}(ff)}{P_{incident}}$$

Based upon the dependencies of the parameters of efficiency on both the device (e.g., shunt resistance, series, resistance, etc.) and the material (minority carrier lifetimes, diffusion lengths, doping concentrations, etc.) properties, it can be seen that both of these aspects play influential roles in determining the performance of a solar cell. The maximum theoretical efficiency which a single p-n junction solar cell can achieve is known as the Shockley-Queisser limit, and for the global solar spectrum (AM1.5) is limited to approximately 33.7% for a solar cell with a bandgap energy near that of GaAs.

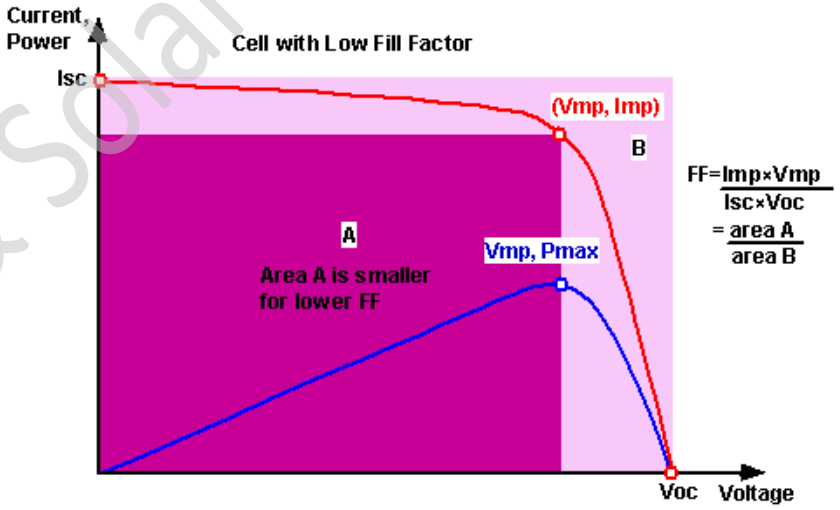


**Figure 5.** *An example plot of the IV (red) and PV (blue) curves of a solar cell, with the dark shaded area corresponding to the fill factor* [8].

In a typical p-i-n solar cell, a region of intrinsic (i.e., undoped) semiconductor material is grown in between the p-type and n-type regions of a p-n junction. This region allows the electric field across the p-region and the n-region to build up and drive the flow of carriers (i.e., current), effectively spurring the power output of the solar cell. However, in a p-i-n junction structure, the solar cell is limited to only absorb photons with energy $E \geq E_g$ while photons of lower energy pass through. One method of expanding the absorption range of a solar cell to include some photons with energy $E < E_g$ is to implement a MQW structure rather than a simple bulk intrinsic region between the p-region and n-region.

A quantum well is a region with discrete levels of potential energy in which charge carriers are only free to move in two dimensions (i.e., restricted to a plane). The discrete energy levels can be derived by solving Schrodinger's equation with the relevant quantum mechanical parameters and boundary conditions. In practice, a quantum well can be realized by depositing a thin layer of semiconductor material in between two layers of another material with a different bandgap energy. Due to the difference in the bandgap energies on either side of the middle layer, a finite quantum well is effectively formed (Figure 6).

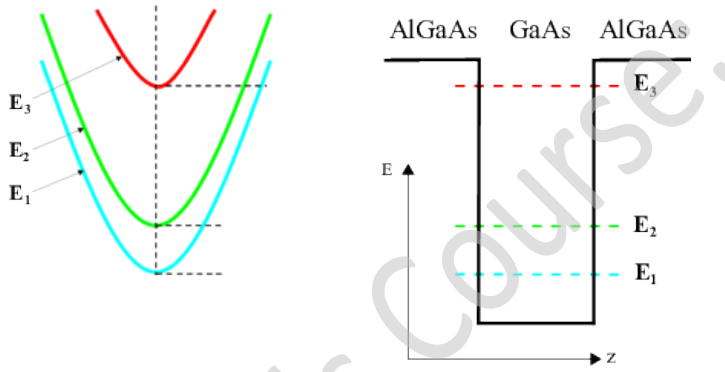


**Figure 6.** *Structure of a GaAs finite quantum well formed in between two AlGaAs barriers* [9].

In a MQW solar cell, several quantum wells are deposited consecutively in the place of the intrinsic bulk semiconductor region in a p-i-n junction (Figure 7). This allows photons with energy $E < E_g$ to be absorbed in the quantum wells to excite electrons and holes so that they can escape from the well and contribute to the current produced by the solar cell [4]. In order for this phenomenon to occur, the voltage must be in between the bandgap voltages of the quantum well and bulk barrier materials. The net result is that the open circuit voltage of the cell slightly decreases in exchange for a significant increase in the short circuit current. Unlike a conventional solar cell where the efficiency decreases at higher temperatures, the efficiency of a MQW solar cell can actually increase at elevated temperatures or under strong optical concentrators due to the thermal activation of carriers in the quantum wells.

When a charge carrier escapes from a quantum well structure, there can also be unintended processes which take place depending on parameters such as voltage and temperature. Typically, if there is a high reverse bias, then the photocurrent generated from the quantum wells is independent of the voltage or temperature. However, at lower reverse biases, the generated photocurrent can become temperature dependent (assuming an environment at or above room temperature) if the energy of the quantum wells is on the order of $\sim k_B T$. At very low temperatures, thermal activation becomes virtually impossible and the photocurrent generated by the quantum wells is dependent only on the voltage.

As it has been previously mentioned, GaAs solar cells are a system of particular interest for MQW designs because they offer the highest potential efficiency as a single junction solar cell. MQW GaAs solar cells of various device configurations and material parameters have been attempted in the past, of which a handful are listed in Table 1. For example, InGaAs/GaAsP quantum wells have been fabricated in an attempt to reduce the dark current of a GaAs solar cell [10]. The alloy compositions can be designed in such a way that the bandgap of the GaAsP barriers exceeds that of GaAs so that the parasitic effects of dark current and thermalization can be suppressed. Another common material choice for MQW structures is

GaAs/AlGaAs in which GaAs serves as the quantum well. For any of these systems, there is a need to optimize many parameters including the number of quantum wells, well depth (i.e., selection of bandgaps for the barrier and the well), well thickness, barrier thickness, barrier composition, and strain at material interfaces.

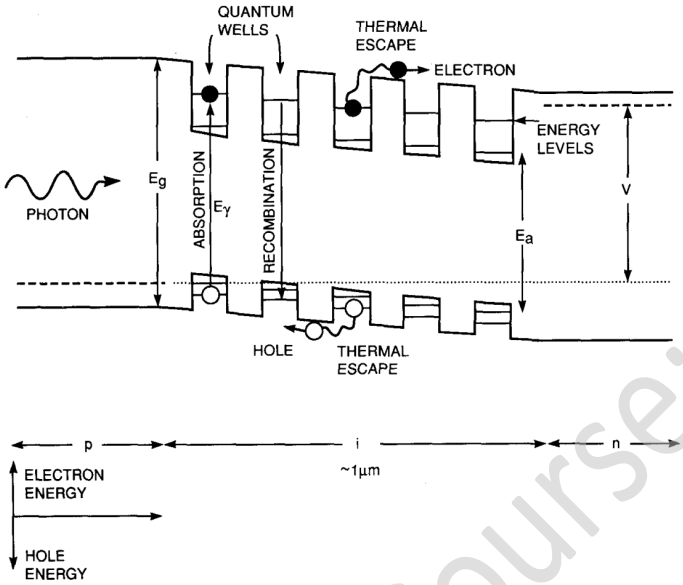


**Figure 7.** *Schematic of the energy levels across a multi-quantum well solar cell* [4].

| Solar Cell | Quantum Well | $V_{oc}$ (V) | $J_{sc}$ (mA/cm$^2$) | AM1.5 Efficiency (%) | Reference |
|---|---|---|---|---|---|
| GaAs | GaAsP/InGaAs | 0.964 | 25.4 | 20.2 | [11] |
| GaAs | AlGaAs/GaAs | 1.18 | - | 15 | [12] |
| GaAs/InGaP | InGaP | - | - | 30.6 | [13] |
| InGap/GaAs/Ge | InGaAs/GaAs | 2.3 – 2.5 | 20-23 | >30 | [14] |

**Table 1.** *Summary of reported MQW solar cells with their device structure and performance metrics.*

## III. Simulation and Results

In this study, two-dimensional simulations of a MQW GaAs solar cell using GaAs/AlGaAs quantum wells are performed using Crosslight APSYS, which is a 2D/3D finite element analysis software used to model semiconductor devices. Finite element analysis is a computational technique used to numerically solve differential equations by dividing a large 2D or 3D problem into many small, simple problems by the construction of a mesh across the problem geometry. The APSYS model functions by numerically solving Poisson's equation, as well as the current continuity equations for electrons and holes as follows [15]:

$$-\nabla\cdot\left(\frac{\varepsilon_0\varepsilon_{dc}}{q}\nabla \mathrm{V}\right) = -n + p + N_D(1-f_D) - N_A f_A + \sum_j N_{tj}\left(\delta_j - f_{tj}\right)$$

$$\nabla\cdot J_n - \sum_j R_n^{tj} - R_{sp} - R_{st} - R_{au} + G_{opt}(t) = \frac{\partial n}{\partial t} + N_D\frac{\partial f_D}{\partial t}$$

$$\nabla\cdot J_p + \sum_j R_p^{tj} + R_{sp} + R_{st} + R_{au} - G_{opt}(t) = -\frac{\partial p}{\partial t} + N_A\frac{\partial f_A}{\partial t}$$

The device structure of the MQW GaAs solar cell simulated in this study is depicted in Figure 8. The cell utilizes 13 quantum wells of GaAs ($N_A = 5.0 \times 10^{11}$ cm$^{-3}$) with $Al_{0.35}Ga_{0.65}As$ as the barrier material. The device consists of 13 quantum wells sandwiched between a 0.5 µm GaAs n-doped base ($N_D = 2.0 \times 10^{19}$ cm$^{-3}$) and a 0.5 µm GaAs p-doped layer ($N_A = 5.0 \times 10^{19}$ cm$^{-3}$). A 50 nm $Al_{0.49}Ga_{0.51}As$ window layer is deposited on top of the p-GaAs layer and is connected to the top ohmic contacts of the cell. The window layer is also p-doped with an acceptor concentration of $N_A = 7.0 \times 10^{19}$ cm$^{-3}$. The window layer can help to reduce the rate of recombination of electron hole pairs in the junction before the carriers are able to diffuse to the contacts to conduct a current out of the solar cell. This in effect can help to reduce the series resistance, $R_s$, of the solar cell in the single diode equivalent circuit model.

The thickness of the quantum wells and the barriers in the MQW region are essential design parameters which were investigated for the outlined device to optimize the cell efficiency. To evaluate the performance of the cell, simulations were performed under a single sun of illumination using the AM1.5 solar spectrum with measurements being taken for reverse biases up to -1.5 V. In order to optimize both of these parameters (the GaAs quantum well thickness and the $Al_{0.35}Ga_{0.65}As$ barrier thickness), each one was varied independently while the other was held constant to observe their effects on the cell efficiency.

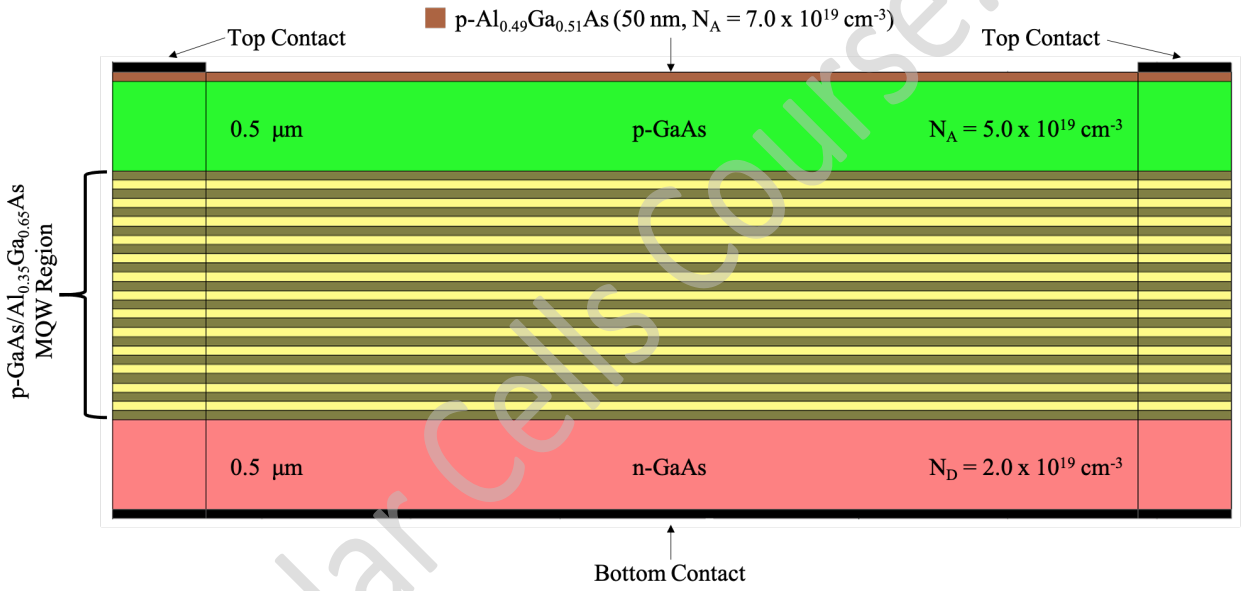


**Figure 8.** *Schematic of the MQW GaAs/AlGaAs solar cell design being simulated in this study.*

In order to determine the optimal thickness of the $Al_{0.35}Ga_{0.65}As$ barrier, a 20 nm GaAs quantum well thickness was assumed. Using the aforementioned solution conditions, the Voc, Jsc (short circuit current density), maximum power output, fill factor, and efficiency were determined to evaluate the device performance. The barrier thickness was varied between 1 – 30 nm, with the results summarized in Table 2.

| $Al_{0.35}Ga_{0.65}As$ Barrier Thickness (nm) | $V_{oc}$ (V) | $J_{sc}$ (A/m$^2$) | $P_{max}$ (W/m$^2$) | Fill Factor (%) | AM1.5 Efficiency (%) |
|---|---|---|---|---|---|
| 1 | 1.003 | 130.083 | 57.496 | 44.054 | 5.967 |
| 5 | 1.000 | 115.187 | 52.242 | 45.342 | 5.422 |
| 10 | 0.996 | 101.112 | 47.838 | 47.496 | 4.965 |
| 20 | 0.990 | 84.704 | 42.962 | 51.209 | 4.459 |
| 30 | 0.986 | 75.511 | 39.968 | 53.673 | 4.148 |

**Table 2.** *Simulation results for varying $Al_{0.35}Ga_{0.65}As$ barrier thicknesses when the GaAs quantum well thickness is fixed at 20 nm.*

From these results, it could be observed that reducing the thickness of the $Al_{0.35}Ga_{0.65}As$ layers increased the efficiency and the maximum power output of the cell. Therefore, a barrier thickness of 1 nm was selected for the device. While these results suggest that making the $Al_{0.35}Ga_{0.65}As$ layers thinner could further enhance the cell efficiency, thicknesses less than 1 nm would be impractical for a real device. Making the barrier layers thinner would increase the probability of electrons tunneling between quantum wells and would theoretically approach the behavior of a conventional p-i-n solar cell without an actual MQW region. Thinner layers would also be far more difficult to fabricate and would require a finer mesh to be defined in the simulation, which can significantly increase computation times or cause the model to fail to converge to a numerical solution. However, for the purpose of this study, a barrier thickness of 1 nm was utilized to observe the performance of the solar cell design.

Next, the thickness of the GaAs quantum well was varied between 5 – 100 nm with the barrier thickness fixed at 1 nm (Table 3). The relationship between quantum well thickness and efficiency is less direct than that of the barrier thickness, as can be observed in Figure 9. The cell efficiency is maximized at a value of 7.64% for a quantum well thickness of 50 nm. The $V_{oc}$, $J_{sc}$, and maximum power follow similar trends to that of the efficiency with respect to the quantum well thickness.

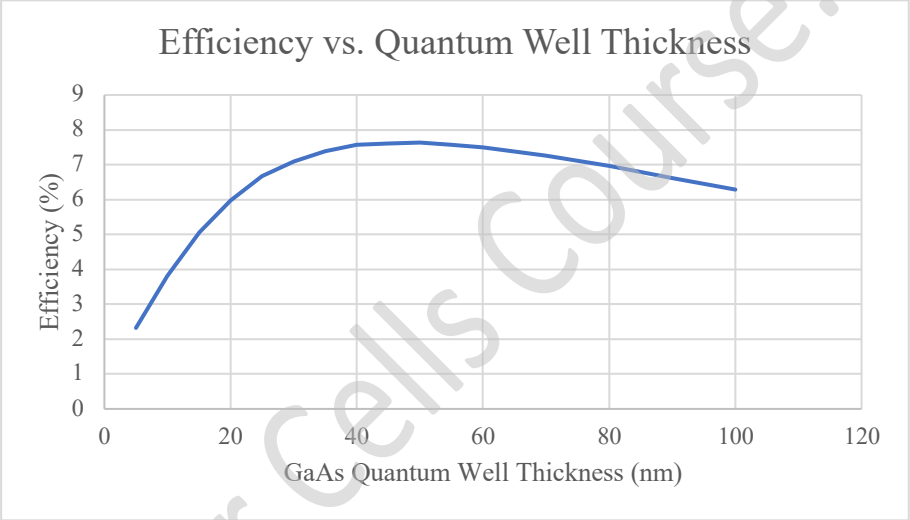


**Figure 9.** *Plot of solar cell efficiency computed in simulations vs. quantum well thickness for the MQW GaAs/AlGaAs design being studied.*

| GaAs Quantum Well Thickness (nm) | $V_{oc}$ (V) | $J_{sc}$ (A/m$^2$) | $P_{max}$ (W/m$^2$) | Fill Factor (%) | AM1.5 Efficiency (%) |
|---|---|---|---|---|---|
| 5 | 1.035 | 74.783 | 22.346 | 28.867 | 2.319 |
| 10 | 1.023 | 101.433 | 36.663 | 35.347 | 3.805 |
| 15 | 1.012 | 119.190 | 48.670 | 40.344 | 5.051 |
| 20 | 1.003 | 130.083 | 57.496 | 44.054 | 5.967 |
| 25 | 0.995 | 138.772 | 64.316 | 46.583 | 6.675 |
| 30 | 0.987 | 143.661 | 68.410 | 48.268 | 7.100 |
| 35 | 0.980 | 147.683 | 71.196 | 49.203 | 7.389 |
| 40 | 0.972 | 151.184 | 73.013 | 49.695 | 7.577 |
| 45 | 0.965 | 152.584 | 73.355 | 49.823 | 7.613 |
| 50 | 0.959 | 154.578 | 73.578 | 49.639 | 7.636 |
| 55 | 0.952 | 155.055 | 72.883 | 49.376 | 7.564 |
| 60 | 0.946 | 156.320 | 72.306 | 48.889 | 7.504 |
| 70 | 0.935 | 156.799 | 69.944 | 47.707 | 7.259 |
| 80 | 0.925 | 156.737 | 67.139 | 46.324 | 6.968 |

| | | | | | |
|---|---|---|---|---|---|
| 90 | 0.915 | 155.725 | 63.855 | 44.815 | 6.627 |
| 100 | 0.906 | 154.615 | 60.607 | 43.272 | 6.290 |

**Table 3.** *Simulation results for varying GaAs quantum well thicknesses when the $Al_{0.35}Ga_{0.65}As$ barrier thicknesses are fixed at 1 nm.*

Based on these results, a quantum well thickness of 50 nm was selected for the solar cell. The solar cell has a $V_{oc}$ of 0.959 V, a $J_{sc}$ of 154.6 A/m$^2$, a fill factor of 49.6%, and an efficiency of 7.636%. These parameters can be determined and verified from the IV curve of the solar cell (Figure 10). The energy band diagram for this device is also determined by the model (Figure 11). The quantum wells can easily be observed and counted by the 13 small "peaks" in the band diagram. In addition, the relative energy density can be plotted as a function of spatial position in the cell (Figure 12). It can be observed here that the energy absorbed is highest at the window layer of the cell and lower in the MQW region. This trend is expected, as the majority of the generated carriers are produced by light absorption in the junction rather than excitation of carriers in the quantum well region. However, the energy density is still quite low in the quantum well region, indicating that this solar cell design has further need for optimization.

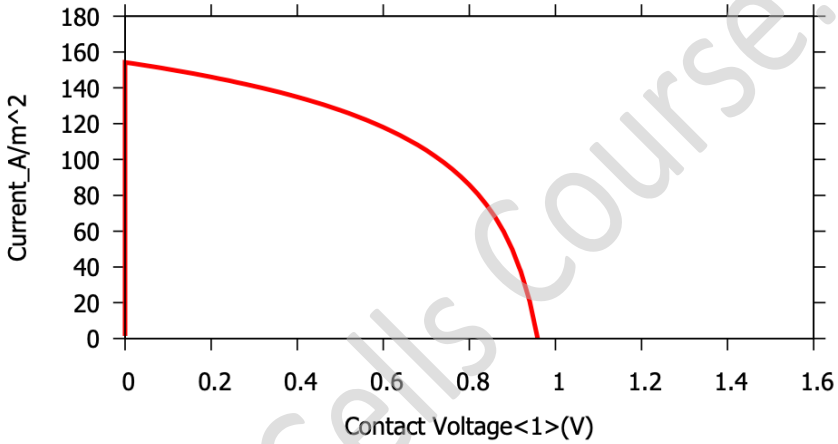


**Figure 10.** *IV curve of the MQW GaAs/AlGaAs solar cell.*

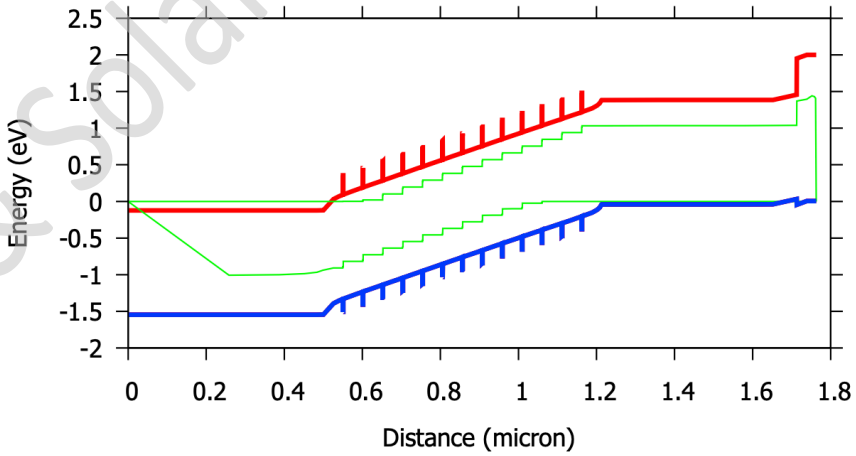


**Figure 11.** *Energy band diagram of the MQW GaAs/AlGaAs solar cell.*

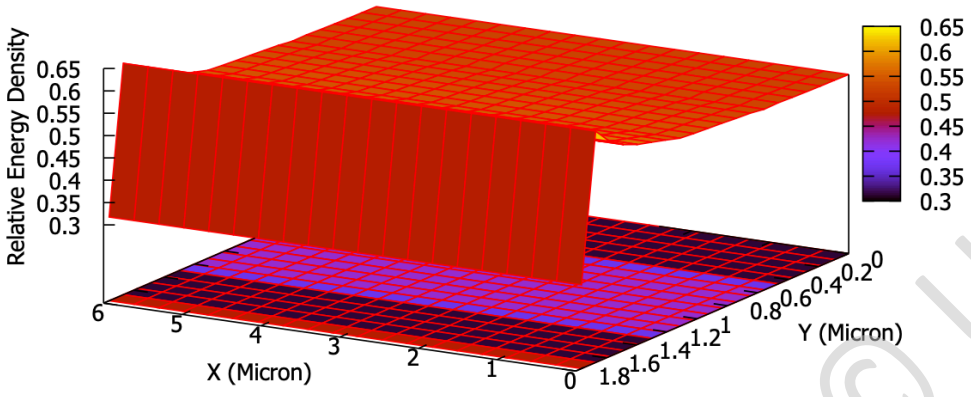


**Figure 12.** *3D surface plot of the relative energy density across the 2D plane of the MQW GaAs/AlGaAs solar cell.*

Overall, the performance of the MQW GaAs/AlGaAs solar cell is consistent with the fundamental physical principles which govern solar cell operation. However, the peak efficiency achieved by this design in the described simulation parameters is only 7.636%; a fraction of the peak efficiency and the Shockley-Queisser limit for a GaAs solar cell. One factor which may have limited the efficacy of the quantum wells is the thickness of the barrier layers. The barriers were only 1 nm thick in this study, which is likely thin enough for carrier tunneling between the quantum wells to dominate over the excitation of carriers out of the quantum well to generate a current output. If the quantum well thicknesses were scaled to be closer to the thickness of the barrier, the energy levels of the quantum well would increase. This effect is also undesirable as photons of higher energy levels would be needed to promote the excitation of free carriers in the MQW region. This would counteract the original purpose of the MQW region, which is to encourage current generation by absorbing photons which otherwise would not be utilized in a conventional p-i-n structure. This trade-off reflects the complexity of optimizing the MQW system, as there are also many other degrees of freedom which must be taken into account such as the ideal number of quantum wells and the composition (and in effect, the bandgap) of the AlGaAs alloys.

## IV. Summary and Conclusion

In this study, the operation of a MQW GaAs/AlGaAs solar cell is successfully executed to gain insights into the limitations and viability of such a device structure. The proposed design did function as a solar cell with 7.636% conversion efficiency, but its performance still pales in comparison to state-of-the-art high performance GaAs single junction solar cells. Despite this, the concept still deserves further attention for its potential to enhance the current generated in III-V solar cells. In particular, for solar cells used in space exploration and other niche applications requiring high efficiencies, the added value of generating more current using quantum wells can provide a needed boost both in single junction and multijunction devices. A similar structure can be attempted for cell designs other than GaAs/AlGaAs where the current may be a limiting factor to the performance.

With respect to the quantum well design, there are many free parameters which need to be optimized. One of the most obvious ones which was not explored in great depth in this study is the number of quantum wells in the MQW region. For any given number of quantum wells, the optimal value of other parameters such as the barrier and well thicknesses will shift, thus requiring further simulations to iteratively determine the best device structure. While in this study, the number of simulations which could be performed was limited, it could be of interest in future studies to execute a large number of simulations across the space of tunable independent variables such as the barrier thicknesses, well thicknesses, and alloy compositions for several different numbers of quantum wells. This data could be used to train a machine

learning model to determine design rules for MQW solar cells so that future studies can be accelerated by focusing on a subset of more important parameter ranges. Alternatively, machine learning models could also be used in tandem with fundamental quantum mechanical calculations to identify material parameters for the ideal MQW solar cell to maximize the additional current generation. However, this process would be highly computationally expensive and time-consuming.

The results produced in this study also have room for improvement through the defined simulation parameters. For example, the tolerances of the Newton solver were increased from their default parameters in order to avoid non-converging simulation results. This expectedly results in a loss of precision in the simulated performance metrics of the solar cell. The mesh also could have been further optimized to produce more precise results, although this would come at the expense of computation time. The Crosslight APSYS model is also very sensitive to small changes in alloy compositions, which limits the range of AlGaAs compositions that can be explored without compromising the precision through larger solution tolerances, increased damping factors, or oversimplified material characteristics.

Aside from the simulation parameters, there are many other paths which can be explored with the available modeling tools to improve on the MQW solar cell in the future. More simulations should be performed using higher barrier thicknesses to determine with greater confidence the point at which quantum tunneling begins to overtake carrier excitation in the MQW region and what minimal thickness and material parameters are needed to avoid its limitation on the generated current extracted from the quantum wells. The optimization of the barrier alloy composition was also not fully explored in this study and warrants further attention, as it ultimately affects the determination of the energy levels for the quantum wells. Quantum well systems other than GaAs/AlGaAs can also be considered, although if they are to be used within a GaAs single junction solar cell, issues of strain due to lattice mismatches must also be considered. There could also be more engineering done with the quantum wells by using layers of varying thicknesses or compositions rather than a uniform stack of the same well repeated across a period. However, this would increase the complexity of the device fabrication and could make identification of problem sites difficult. Lastly, further experimentation to determine the optimal number of quantum wells for the solar cell performance would provide much needed insights into the potential viability of these systems. If these parameters can be optimized for a single junction solar cell, then this could provide an exciting boost to the performance of multijunction solar cells if the same design principles can be carried over.

## V. References


[1] R. Eisenberg and D. G. Nocera, "Preface: Overview of the forum on solar and renewable energy," *Inorg. Chem.*, vol. 44, no. 20, pp. 6799–6801, 2005, doi: 10.1021/ic058006i.

[2] M. Woodhouse *et al.*, "On the Path to SunShot: The Role of Advancements in Solar Photovoltaic Efficiency, Reliability, and Costs," *Natl. Renew. Energy Lab.*, no. May, p. 44, 2016, [Online]. Available: http://www.osti.gov/scitech/biblio/1253983.

[3] A. Polman, M. Knight, E. C. Garnett, B. Ehrler, and W. C. Sinke, "Photovoltaic materials: Present efficiencies and future challenges," *Science (80-. ).*, vol. 352, no. 6283, 2016, doi: 10.1126/science.aad4424.

[4] K. Barnham, J. Barnes, J. Nelson, M. Paxman, T. Foxon, and J. Roberts, "Quantum-Well Solar Cells," *MRS Bull.*, no. OCTOBER 1993, pp. 51–55, 1993.

[5] O. K. Simya, P. Radhakrishnan, A. Ashok, K. Kavitha, and R. Althaf, "Engineered nanomaterials for energy applications," *Handb. Nanomater. Ind. Appl.*, pp. 751–767, 2018, doi: 10.1016/B978-0-12-813351-4.00043-2.

[6] J. Weisse, "Concentrated Solar Photovoltaics," *Stanford University*, 2010. http://large.stanford.edu/courses/2010/ph240/weisse2/.

[7] PVPerformance, "Single Diode Equivalent Circuit Models," *Sandia National Laboratories*, 2016. http://pvpmc.org/modeling-steps/module-iv-curve/diode-equivalent-circuit-models/.

[8] C. Honsberg and S. Bowden, "Solar Cell Operation - Fill Factor," *PVEducation*, 2020.

[9] M. Moradinasab, "Optical Properties of Semiconductor Nanostructures," Technical University at

Vienna, 2015.
[10] M. Mazzer *et al.*, "Progress in quantum well solar cells," *Thin Solid Films*, vol. 511–512, pp. 76–83, 2006, doi: 10.1016/j.tsf.2005.12.120.
[11] A. You, M. A. Y. Be, and I. In, "Strain-balanced GaAsP / InGaAs quantum well solar cells," *Appl. Phys. Lett.*, vol. 4195, no. December 1999, pp. 1–4, 2001.
[12] J. C. Rimada, L. Hernandez, J. P. Connolly, and K. W. J. Barnham, "Quantum and conversion efficiency calculation of AlGaAs/GaAs multiple quantum well solar cells," *Phys. Status Solidi Basic Res.*, vol. 242, no. 9, pp. 1842–1845, 2005, doi: 10.1002/pssb.200461764.
[13] J. G. J. Adams *et al.*, "Recent results for single-junction and tandem quantum well solar cells," *25th EU PVSEC WCPEC-5*, pp. 865–867, 2011, doi: 10.1002/pip.
[14] A. Freundlich and A. Alemu, "Multi quantum well multijunction solar cell for space applications," *Phys. Status Solidi C Conf.*, vol. 2, no. 8, pp. 2978–2981, 2005, doi: 10.1002/pssc.200460720.
[15] Z. Q. Li, Y. G. Xiao, and Z. M. S. Li, "Modeling of multi-junction solar cells by Crosslight APSYS," *High Low Conc. Sol. Electr. Appl.*, vol. 6339, no. September 2006, p. 633909, 2006, doi: 10.1117/12.681258.